Contract Information

Contract Number	N00014-15-1-2445
Title of Research	Investigating the Effects of Service History on Al Ship Plates
Principal Investigator	John J Lewandowski
Organization	Case Western Reserve University

Technical Section

Technical Objectives

The present work had intended to systematically investigate the effects of 42-year service history on the mechanical properties of various Al-Mg alloy plates removed from the HMCS *Iroquois*. Although the PI has visited Halifax, Nova Scotia where the *Iroquois* was docked in preparation for removal of plates from various sections, the removal of such plates was delayed in Halifax and testing of such plates only occurred in the last year of the grant. In order to continue to make progress in related areas and provide a related educational and research experience for an excellent domestic student, Benjamin Palmer, we also obtained some pedigree material, 5083-H131, in order to enable him to complete his MS Thesis. This enabled the experiments on 5083-H131 to be compared to the preliminary expereiments conducted on plates from the HMCS *Iroquois* material when it arrived in the third year of the grant. In particular, CWRU has determined the changes in failure mode, strain accommodation, and mechanical properties of 5083-H131 at a variety of thermal exposure times/temperatures under humid and dry environments. Though a large body of research has been done at Case Western Reserve University and other institutions to investigate the effects of thermal exposure on the properties of 5XXX alloys (e.g. mechanical, electrochemical, etc.), less work has been done to investigate the mechanisms behind these trends, and very little work has been conducted on material removed from service. Service material from the HMCS *Iroquois* was tested in the third year of the grant in addition to conducting work in a follow-on grant that will start in July 2018.

The completed work has determined the changes in failure mode, strain accommodation, and mechanical properties of 5083-H131 rolled plate at a variety of thermal exposure times/temperatures under humid and dry environments. Through the work, a previously identified type of environmentally enhanced cracking was observed at strain rates two orders of magnitude higher than other experiments. Additionally, it was shown that there is a change in strain heterogeneity within the material due to thermal exposure. Differential Scanning Calorimetry (DSC) was used to detect the evolution of phase(s) at thermal exposures as low as 60°C, and applied to determine the efficacy of different remediation treatments in reducing the effects of thermal exposure. Similar DSC studies have been performed on a few plates from the HMCS *Iroquois* material. Additional work will be conducted on the remaining plates in a new follow on grant to start in July 2018.

REPORT DOCUMENTATION PAGE	*Form Approved* *OMB No. 0704-0188*

1. REPORT DATE *(DD-MM-YYYY)*	**2. REPORT TYPE**	**3. DATES COVERED** *(From - To)*
5/24/2018	Final Report	April 20, 2015 - April 17, 2018

4. TITLE AND SUBTITLE
Investigating the Effects of Service History on Al Ship Plates

5a. CONTRACT NUMBER

5b. GRANT NUMBER
ONR-N00014-15-1-2445

5c. PROGRAM ELEMENT NUMBER

6. AUTHOR(S)
John J Lewandowski

5d. PROJECT NUMBER

5e. TASK NUMBER

5f. WORK UNIT NUMBER

7. PERFORMING ORGANIZATION NAME(S) AND ADDRESS(ES)
Case Western Reserve University

8. PERFORMING ORGANIZATION REPORT NUMBER

9. SPONSORING/MONITORING AGENCY NAME(S) AND ADDRESS(ES)
Office of Naval Research
875 N. Randolph Street, Suite 1425
Arlington, VA 22203-1995

10. SPONSOR/MONITOR'S ACRONYM(S)

11. SPONSOR/MONITOR'S REPORT NUMBER(S)

12. DISTRIBUTION/AVAILABILITY STATEMENT
Approved for Public Release; Distribution is Unlimited

13. SUPPLEMENTARY NOTES

14. ABSTRACT
The work involved a systematic study to determine the effects of changes in thermal exposure conditions (i.e. time, temperature), and environment (e.g. dry air, humid air, solutions) on the environmental cracking susceptibility of 5083-H131 alloy plate. Experiments were conducted using slow strain rate tension (SSRT) and fatigue crack growth using dcPD to determine the effects of changes in loading rate on cracking susceptibility. In addition, access to high-resolution tomography occurred via a visit to the Harwell Diamond Light Source (DLS), UK, where in-situ cracking experiments were conducted as well as tomography experiments on previously tested samples. In addition, Al-Mg alloy plates were retrieved in the third year of the grant from the HMCS Iroquois after 42-year service. Preliminary experiments were conducted on these plates in a manner similar to that conducted on the 5083-H131.

15. SUBJECT TERMS
Al-Mg alloys, Environmentally Assisted Cracking (EAC), Slow Strain Rate Testing (SSRT), Fatigue Crack Growth (FCG), HMCS Iroquois

16. SECURITY CLASSIFICATION OF: a. REPORT	**b. ABSTRACT**	**c. THIS PAGE**	**17. LIMITATION OF ABSTRACT**	**18. NUMBER OF PAGES**	**19a. NAME OF RESPONSIBLE PERSON**
U	U	U	UU	13	John Lewandowski
					19b. TELEPHONE NUMBER *(Include area code)* 216 368 4234

Reset

The first objective of the work, in the initial absence of the HMCS *Iroquois* material, was to determine the effect of a 'service-like' environment, i.e. humid air, on the failure mode of pedigree material. Other work at Case Western Reserve University has shown unexpected damage phenomena in thermally exposed 5XXX alloys, such as grain bounday splitting in the ST plane during fatigue crack growth tests. These phenomena may be enhanced where highly aggressive environments (e.g. full submersion in NaCl solution) are used. A second objective was to investigate the effects of thermal exposure and environment upon strain accommodation. It is known from prior work that both can have an effect on global mechanical properties, so it is of interest to determine if this transfers to microscale phenomena. The third objective was to explore the use of DSC as an additional metric for the Degree of Sensitization (DoS) of thermally exposed 5XXX alloys. These were conducted to complement the Nitric Acid Mass Loss Test (NAMLT), as the NAMLT test it is known to have several issues and cannot be readily applied to service material due to the large required sample size and limited thickness (i.e. 0.25") of the service material. However, NAMLT tests were conducted on sub-sized HMCS *Iroquois* plate material and the results were normalized with respect to the area/volume utilized. Testing of the HMCS *Iroquois* plate materials will continue with the new grant starting in July 2018.

Technical Approach

Tensile specimens used in this study were taken from 29.2 mm (1.15 in) thick 5083-H131 cold-rolled plates. Similar intial testing has been conducted on the HMCS *Iroquois* plate material, adjusted for plate thickness. The microstructure of the 5083-H131 consisted of 35 μm x 80 μm x 150 μm pancake-shaped grains (measured in accordance with ASTM E112), elongated in the rolling direction. The chemical composition was approximately 4.46 wt% Mg, 0.62 wt% Mn, 0.08 wt% Cr, 0.02 wt% Ti, 0.07wt% Si, 0.12 wt% Fe, 0.02 wt% Zn, and the balance Aluminum. Dogbone tensile specimens were machined with the tensile axis parallel to the Short-Transverse (S-T) direction of the plate with a 6.35 mm (0.25 in) gauge and 4.45 x 3.81 mm (0.175 x 0.15 in) cross section. The samples were tested in the As-Received (AR) condition, thermally exposed at 175°C for 100 hrs, and at 800°C for 500 hrs and 1500 hrs. Testing was performed under either a humid (40-50% Relative Humidity (RH)) environment via a humidifier or a dry (<1% RH) environment by surrounding the sample in Magnesium Perchlorate desiccant to determine the environmental effects. Some of the specimens were additionally pre-soaked in de-ionized water at room temperature (~20°C) for 100 hrs to produce increased hydrogen charging within the material.

Samples of the 5083-H131 underwent interrupted tensile testing, whereby a polished side of the sample was imaged using optical microscopy before testing, then the sample was sequentially strained to 1%, 3%, and 6% plastic strain/failure, imaging the same location between each interval. The fracture surfaces were imaged using a Zeiss Axioplan 2 top-down optical microscope, in scanning electron microscopy (SEM) using a FEI Quanta 200 3D SEM, and in 3D optical profilometry with a Keyence Olympus VHX 5000 microscope. Optical and SEM measurements were used to determine the failure mode/morphology of the specimens, while the optical profilometry supplied complementary 3D data (crack depth, roughness, etc.)

Differential Scanning Calorimetry (DSC) specimens of 15-25 mg were cut from legacy samples of the same material, thermally exposed at temperatures of 60°C, 80°C, 100°C, and 175°C at times ranging from 1 hr to 20,000 hrs. Scans were performed at a heating rate of 5°C/min in a Netzch 404 F1 Pegasus DSC machine. Baseline tests on empty sample holders were performed beforehand for each scan pattern to correct for the background effects. Peaks corresponding to the dissolution of Magnesium-rich phase(s) were identified by complimentary Netzch software on the data recording computer. Similar preliminary experiments have been conducted on the HMCS *Iroquois* plate material.

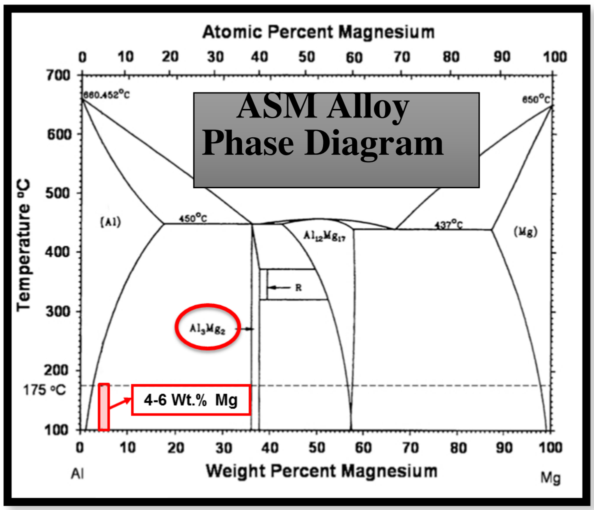

Figure 1: Al-Mg phase diagram showing typical Mg range for 5456, 5083, and 5059 alloys as well as Mg-rich equilibrium phase that can evolve at grain boundaries during sensitization.

Although 5083/5XXX alloys are not precipitation hardened, the exposure of these materials at intermediate test temperatures for long periods of time results in the precipitation of a Mg-rich phase at the grain boundaries, Figure 1. The completed work on pedigree 5083-H131 has shown the effect of environment and thermal exposure in producing three different types of failure in the tensile specimens at intermediate strain rates ($\dot{\varepsilon} = 10^{-3}$/s): two environmentally enhanced cracking phenomena, and one non-environmental one. The specimens also displayed a drop in the yield strength and Ultimate Tensile Strength (UTS) upon thermal exposure, and additional reductions to the UTS and strain to failure when thermally exposed samples were tested in a humid environment. These agree with preliminary thermodynamic models and changes in the failure mode upon environmental testing. Interrupted tensile tests showed a difference in strain accommodation due to thermal exposure both qualitatively (via optical microscopy) and quantitatively (via surface roughness measurements).

Work in the third year of the grant was extended to test samples taken from the decommissioned HMCS *Iroquois*, having 42 years of service exposure, and recently received at CWRU. As indicated earlier, testing of the HCMS *Iroquois* plate material has been delayed due to setbacks in obtaining the material from Halifax, Nova Scotia.

Representative stress-strain curves from the 5083-H131 samples showing changes due to thermal and environmental exposure are shown in Figure 2. As seen in other studies, there is an initial drop in the yield strength and UTS upon thermal exposure. Thermodynamic models using JMAK and diffusional kinetics were used to approximate these reductions via magnesium depletion in the matrix from precipitating intergranular Magnesium-rich phase(s). The results agreed with values in the present study and other ones, indicating that this is a plausible mechanism for strength reduction. Further reductions in the UTS and strain to failure were observed in samples with higher thermal exposures tested in a humid (50%RH) environment. This accords with a change in failure mechanism as described below.

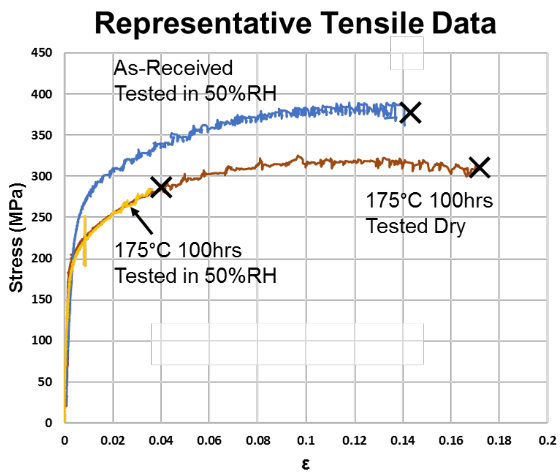

Figure 2: Representative stress-strain curves of the different conditions tested for 5083-H131.

Figure 3 shows the different fracture modes observed on the surfaces of AR/dry-tested 5083-H131 specimens and those tested at higher thermal exposures in a humid environment. In contrast to the ductile shear overload for AR/dry specimens (Figure 3a), the exposed and humid-tested samples show two different environmentally enhanced cracking modes (Figure 3b). One of these is a flat, intergranular crack originating from the surface and consistent with Stress Corrosion Cracking (SCC) and denoted 'Type I' cracking (Figure 4a). The rest of the cracking proceeds by a highly topological mechanism, consisting of a series of plateaus decorated by intermetallic particles (e.g. $Al_6(Mn/Fe)$) and connected with shear walls parallel to the tensile axis (Figure 4b). This is denoted 'Type II' cracking for convenience. In comparison to other studies such as that by *Holroyd et al.* and different environmental cracking mechanisms, it is postulated that this is due to atomic Hydrogen segregating to and embrittling the intermetallic particles. As these enter the crack tip's plastic zone, they themselves crack to produce internal flaws. Some of them grow and eventually link up with the crack tip via shear walls from local overload. This mechanism would give both the observed topology and explain the higher stress intensity required to propagate Type II cracks as compared to Type I cracks.

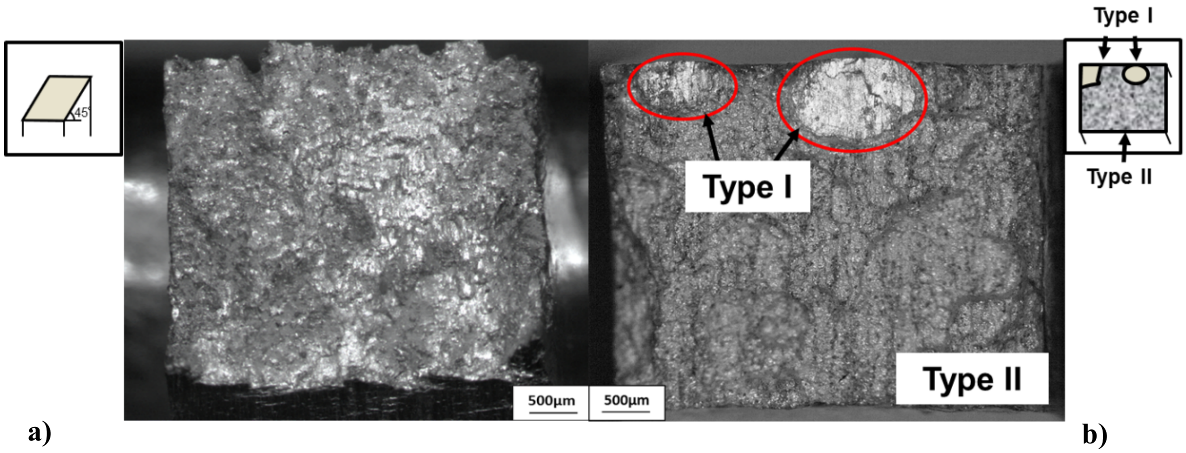

Figure 3: Differences in optical images showing fracture morphologies between (a) AR/dry-tested 5083-H131 samples and (b) sensitized and humid-tested 5083-H131. Type I cracking in (b) is flat and oriented perpendicular to the tensile stress direction.

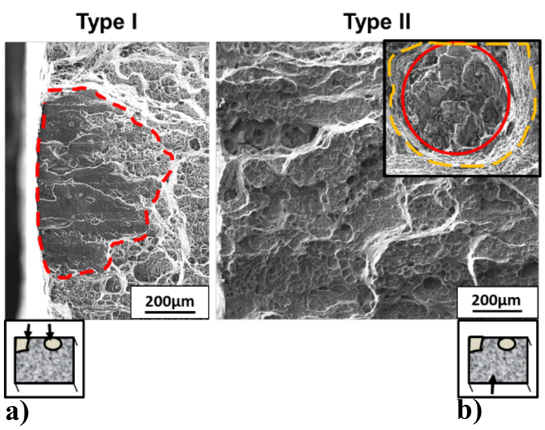

Figure 4: Close-up SEM images of the different environmentally-enhanced cracking modes. a) Type I cracking is flat and oriented perpendicular to the tensile direction. b) Type II cracking is centered on intermetallic particles.

As additional evidence for the proposed mechanism, high-resolution tomography was performed on fractured 5083-H131 specimens showing Types I and II cracking at the Diamond Light Source Synchrotron in collaborative work between the PI and University of Manchester. Using the I13 Diamond Manchester Imaging Branchline, high-energy (8-30 keV), highly-coherent X-rays were used to produce 3D maps of the sample with up to 2 µm feature resolution. This revealed the presence of internal damage below Type II cracks (Figure 5), consistent with the postulated mechanism above.

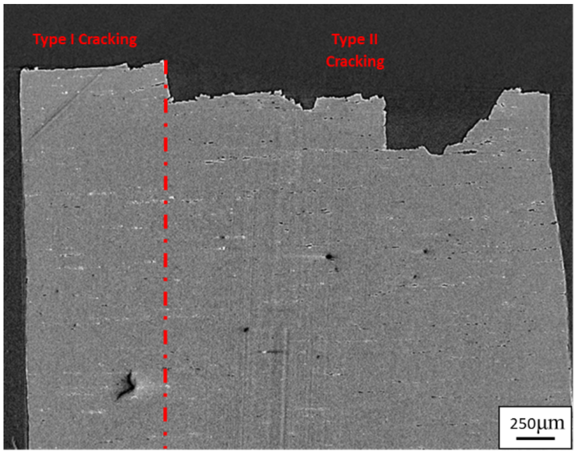

Figure 5: A 2D slice from the tomography scan taken at the Diamond Light Source, UK, of a sample showing Types I and II cracking.

Differences in strain accommodation were also observed across sensitization levels. Figure 6 shows optical images taken during the interrupted tensile testing of an AR 5083-H131 specimen and 175°C, 100 hr specimens tested in humid and dry environments at nominally 6% plastic strain. Qualitatively, the AR specimen shows uniform strain distribution with only a small amount of localization in an x-shaped pattern around an inclusion (Figure 6a). The thermally exposed and humid-tested sample, however, shows a large amount of shear localization/banding on the sample surface. This is indicative of strain localization, producing a ruffled surface topology. The increased topology is more evident with the use of Differential Interference Contrast (DIC) (Figure 6c) which highlights differences in height. Figure 6c also indicates that the change in strain homogeneity is a thermal rather than environmental effect, as it shows similar features despite testing in dry air. Optical profilometry provided a quantitative measure of these trends on the specimens by computing the surface roughness. This gave trends agreeing with the qualitative ones above: AR and less severely exposed 5083-H131 specimens (e.g. 80°C for 500 hrs) had lower roughness vales (RMS = 0.071 and 0.066 respectively) than more highly sensitized 5083-H131 specimens (e.g. 175°C for 100 hrs, RMS = 0.215).

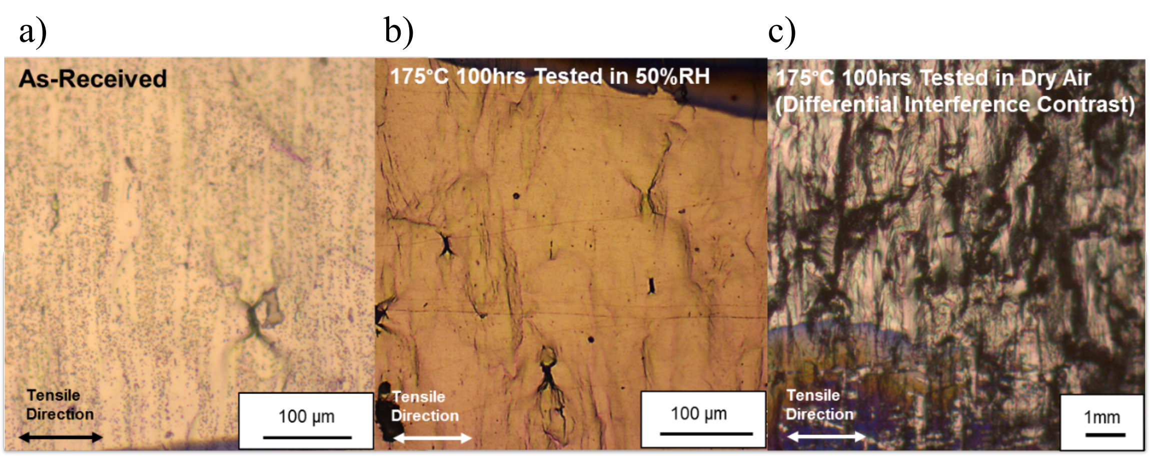

Figure 6: Images of the previously polished surfaces of sequentially strained and unloaded samples after different thermal/environmental conditions. Clear differences in strain homogeneity are evident.

DSC results from the 5083-H131 study were able to find the presence of a Mg-rich phase at thermal exposures as low as 60°C. The DSC peak onset temperature for the dissolution of said phase was consistently ~250°C across different thermal exposure times/temperatures, corresponding to the solvus for equilibrium β (Al_3Mg_2, complex FCC) or its closely-related metastable phase β' (Al_3Mg_2, HCP). As an application of DSC's ability to measure sensitization, 5083-H131 samples that had been thermally exposed at 175°C for 100 hrs were then remediated at two different time/temperature combinations to dissolve precipitated Mg-rich phases: 240°C for 5 hrs and 280°C for 15 mins, as used in other studies. Using the area under the DSC peak as a metric for sensitization level, a reduction in sensitization of approximately 50% was seen upon remediation of the 5083-H131 samples. However, when remediated specimens were additionally re-sensitized under the same conditions (175°C for 100 hrs) there was a 75% *increase* in the sensitization level over the initial thermal exposure. This result indicates that, while thermal remediation may reduce deleterious effects from thermal exposure in the short-term for 5083-H131, it does not provide a long-term solution to the issue. These results will be compared to plate material removed from the HCMS *Iroquois* in the early stages of the new grant starting July 2018.

Initial Work Conducted on HMCS Iroquois Plates

A variety of Al-Mg plates, Figure 7, have been removed from the HMCS *Iroquois* and received at CWRU. Figure 8 summarizes the details regarding each plate with respect to location, dimensions, and likely exposure conditions.

Figure 7: Two Iroquois class destroyers. The HMCS Iroquois (left) with 42 years of service, showing regions from which plates have already been removed and initial testing at CWRU has begun. Material from the HMCS Athabaskan (right) with 45 years of service may become available at some point.

Plate	Size (LxWxt) (in)	Size (LxWxt) (mm)	Width (mm)	Width (in)	Height (mm)	Height (in)	Thickness (in)	Thickness (mm)	Side	For-Aft Location	Exposure	Comments
A	24x16.9x5/8	610x430x15.88	610	24.0	430	16.9	3/8	9.53	Aft Hanger	Aft Hanger Above Door	Bright/ Exposed	Vertical Weld @ 220mm/8.7in from STBD
B	17.7x16.1x5/8	450x410x15.88	450	17.7	410	16.1	3/8	9.53	STBD	2400mm (94.5in) From Aft	Bright/ Exposed	Vertical Weld @ 80mm/3.2in from Aft
C	20.0x16.1x5/8	520x410x15.88	520	20.0	410	16.1	3/8	9.53	STBD	4800mm (189in) From Aft	Bright/ Exposed	Vertical Weld @ 100mm/3.9in from Aft
D	19.7x18.7x5/8	500x500x15.88	500	19.7	500	19.7	3/8	9.53	PORT	1500mm (59in) From Fwd	Bright/ Exposed	Vertical Weld @ 190mm/7.5in from Aft
E	20.1x18.5x5/8	510x520x15.88	510	20.1	520	20.5	3/8	9.53	PORT	5000mm (197in) From Fwd	Bright/ Exposed	
F	20.5x19.7x5/8	520x500x15.88	520	20.5	500	19.7	3/8	9.53	PORT		Bright/ Exposed	Vertical Weld @ 85mm/3.3in from Aft
G	19.7x18.9x5/8	500x480x15.88	500	19.7	480	18.9	3/8	9.53	PORT?	Above Door, Aft Bulk Head	Bright/ Exposed	Vertical Weld @ 190mm/7.5in from STBD Side
H	20.5x20.1x5/8	520x4510x15.88	520	20.5	510	20.1	3/8	9.53	PORT?	Above Door, Aft Bulk Head	Bright/ Exposed	Vertical Weld @ 180mm/7.1in from STBD Side
I	20.1x20.5x1/4	510x520x6.35	510	20.1	520	20.5	1/4	6.35	PORT	Fwd Side of Uptake	Shaded/ Secluded	Vertical Weld @ 15mm/0.6in from Port
J	20.1x21.3x1/4	510x540x6.35	510	20.1	540	21.3	1/4	6.35	STBD	Fwd Side of Uptake	Shaded/ Secluded	
K	15.7x19.7x1/4	400x500x6.35	400	15.7	500	19.7	1/4	6.35	PORT	Funnel Uptake	Shaded/ Secluded	Includes Aluminum Frame and Weld to Steel Deck
L	20.1x19.3x1/4	510x490x6.35	510	20.1	490	19.3	1/4	6.35	STBD	Funnel Uptake	Shaded/ Secluded	Includes Weld to Steel Deck
M	18.9x19.7x5/8	480x500x15.88	480	18.9	500	19.7	3/8	9.53	Port Hanger Top	Port Side of Hangar, Near Aft	Bright/ Exposed	Horizontal Weld @ 150mm/5.9in from Bottom
N	20.1x19.7x5/8	510x500x15.88	510	20.1	500	19.7	3/8	9.53	Port Hanger Top	Port Side of Hangar, Near Aft	Bright/ Exposed	
O	15.7x19.3x5/8	400x490x15.88	400	15.7	490	19.3	3/8	9.53	STBD Hanger Top		Bright/ Exposed	

Figure 8. Details of HMCS Iroquois Al-Mg plates sent to CWRU for testing.

Preliminary testing has been conducted on a few of the plates, with additional testing to resume with a new grant that starts in July 2018. Figure 9 and 10 show a typical plate along with samples removed in different orientations. Tensile testing was conducted in both the L and T orientations in the following environments: Dry, 50% RH, 0.6M NaCl solution, all at 10^{-5}/s. Fatigue crack growth testing was conducted in the L-T orientation for the latter two environments while Rockwell B hardness was additionally conducted. NAMLT tests were conducted on sub-sized samples due to the limited plate thickness.

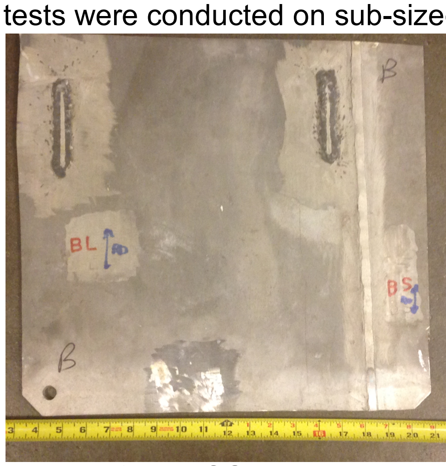

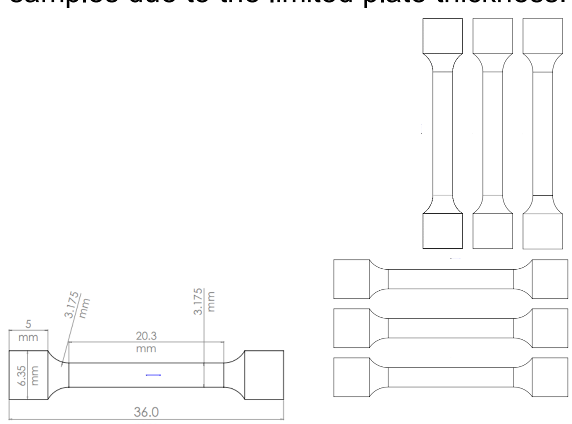

Figure 9. HMCS Iroquois plate. *Figure 10. Tension samples removed from plates.*

Representative results from the preliminary tension tests are shown in Figure 11 with a summary of data collected shown in Figure 12 and the 'spider plots' shown in Figure 13. There are clear differences in the behavior of plates removed from different parts of the ship as well as effects of different environments. Differences in preliminary fatigue crack growth data are in Figure 14.

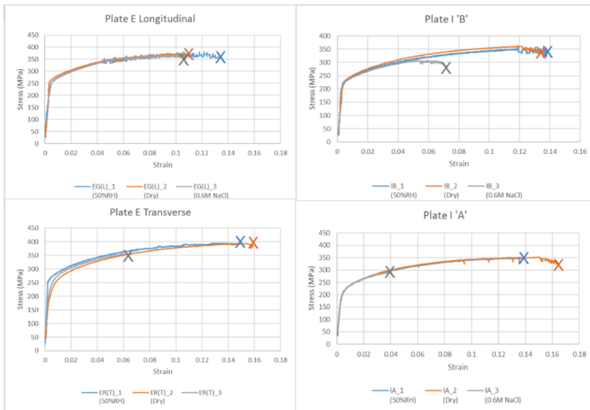

Figure 11. Initial tension results obtained on HMCS Iroquois plate materials.

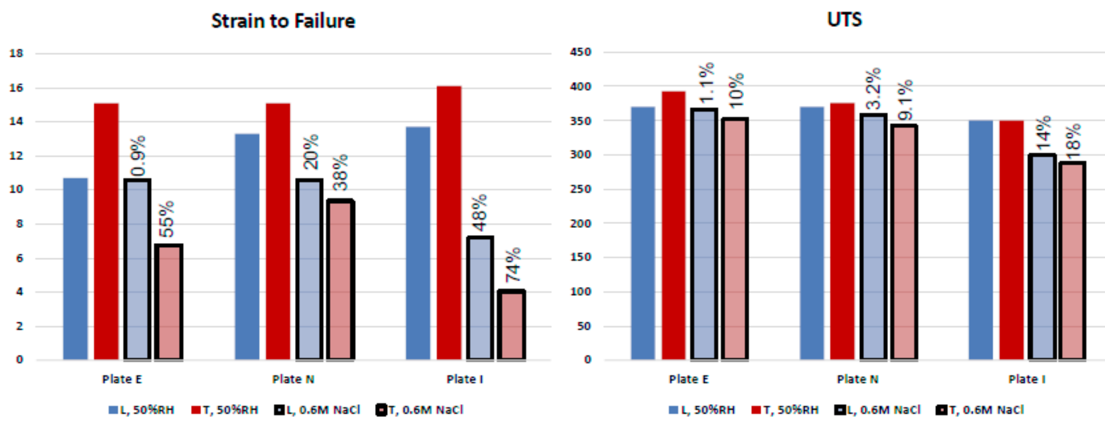

Figure 12. Summary of preliminary tension tests conducted on HMCS Iroquois plates.

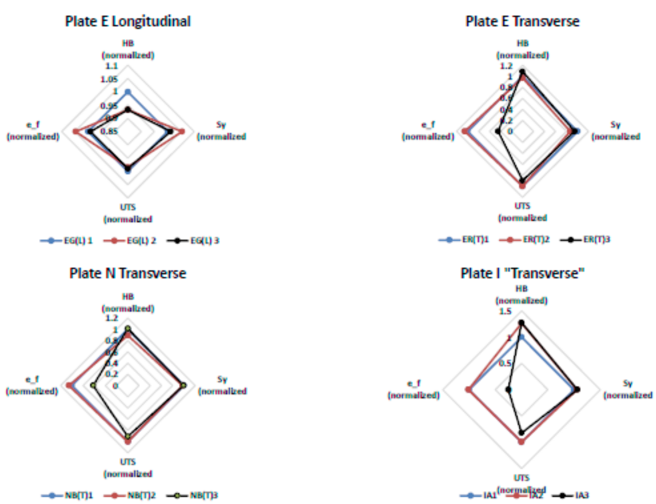

Figure 13. Spider plot summaries of preliminary tension tests on HMCS Iroquois plates.

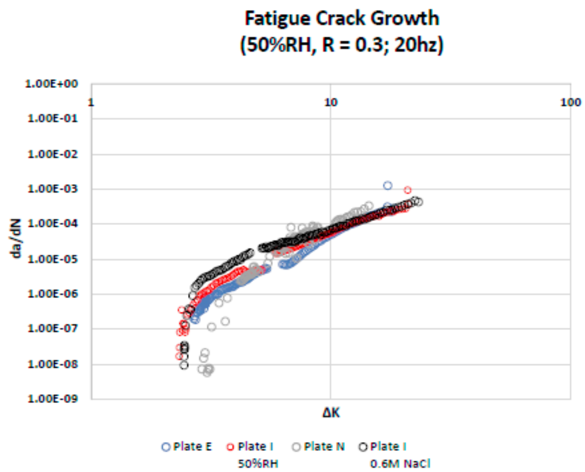

Plate	E	N	I	I
Environs	50% RH	50% RH	50% RH	0.6M NaCl
ΔK_{th} (MPa $m^{0.5}$)	2.7	3.02	2.3	2.45
Paris Slope	3.48	5.07	2.54	2.14
$K_{overload}$ (MPa $m^{0.5}$)	26	20.6	29.9	N/A

Figure 14. Preliminary fatigue crack growth results obtained on HMCS Iroquois plates.

Some differences in the appearances of fracture surfaces were evident for both the tension and fatigue crack growth samples, Figures 15 and 16, respectively. Grain boundary splitting in the ST plane is suggested in the optical images provided in Figure 16. Confirmation will require SEM as conducted in much of our previous work.

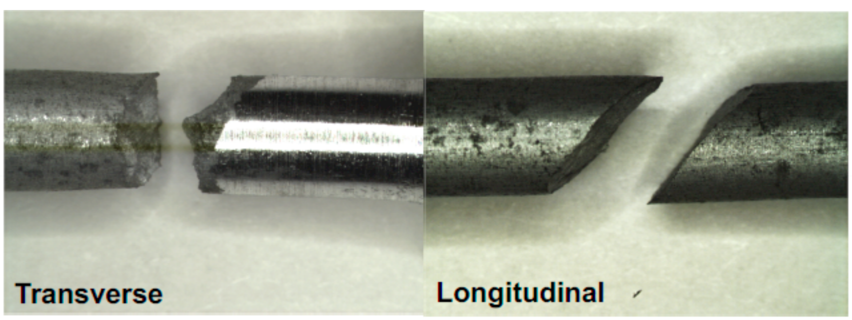

Figure 15. Differences in tensile fracture behavior for T vs L HMCS Iroquois samples.

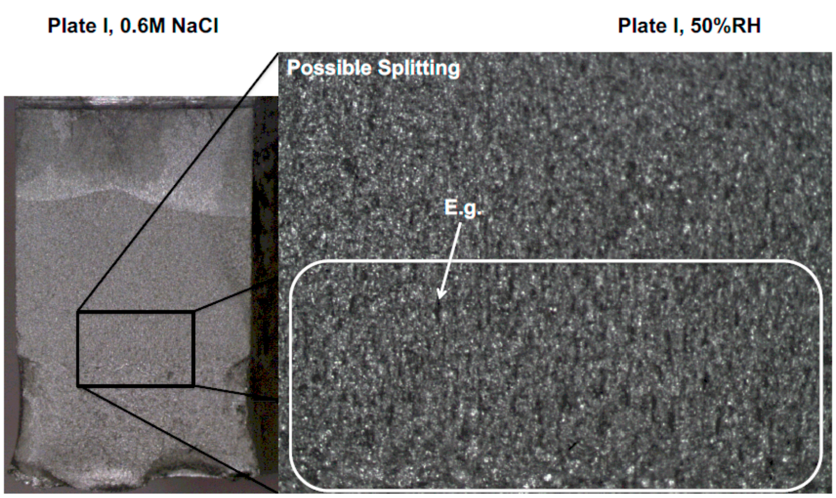

Figure 16. Fatigue crack growth fracture surfaces showing possible grain boundary splitting in the ST plane. SEM will be conducted to confirm.

The work conducted under ONR N00014-15-1-2445 has produced a better understanding of the mechanisms of EAC in 5XXX alloys along with regimes of susceptibility. In addition, preliminary work has been conducted on ship plates removed from the HMCS *Iroquois* after 42-year service. Follow on work is required to complete the work on the HMCS *Iroquois* plate materials. This will be continued in a new grant beginning in July 2018.

Students Supported in this Work

Benjamin Palmer completed his MS project with the funding provided by N000014-15-1-2455 and will continue on for his PhD with new funding that will start on 7/1/18. In addition, Jenna Krynicki, a senior at CWRU, has conducted her senior project on *HMCS Iroquois* plate material in addtion to spending summer 2017 at NSWC working on these and related issues. The early stages of this work received experimental assistance by Dr. Mohsen Seifi. Adjunct Professor Henry Holroyd provided advice during various aspects on the conduct of this work and there were various interactions with Dr. Golumbfskie at NSWC. The PI has visited with all of these collaborators on various occasions.

Presentations Acknowledging N00014-15-1-2445

The following presentations acknowledged the funding provided by N00014-15-1-2445, starting with 2015 and ending with 2018. Fourteen (14) total presentations were made. Three (3) of those presentations were invited and eleven (11) were contributed.

2015 (Designates Invited Talk)**
"Sensitization Effects on Fracture and Fatigue Behavior of Al-Mg Naval Alloys", M. Siefi, H. Jiang, B. Li, and J.J. Lewandowski, 3rd World Congress on ICME, Colorado Springs, CO, June 1, 2015.

2016
**"Environmental Effects on Fracture and Fatigue of Marine Alloys", J.J. Lewandowski, Mini-Symposium on Marine and Offshore Risk Engineering and Advanced Materials-CWRU, Cleveland, OH May 5, 2016.

"Rate-Controlling Processes During Environment-sensitive Crack Propagation in Aluminum', T.L. Burnett, N.J.H. Holroyd, M. Seifi, and J.J. Lewandowski, International Workshop on the Environmental Damage in Structural Materials Under Static Load/Cyclic Loads at Ambient Temperatures", Engineering Conferences International, Cork, Ireland, June 1, 2016.

**"Microstructure-Property Relationships in Advanced Materials", J.J. Lewandowski, MSNO Fall Meeting, Materials Park, OH, October 5, 2016.

2017
"Sensitization Effects on Tensile Behavior in 5XXX Series Aluminum Alloys: Macro- and Mesoscale Observations " B. Palmer and J.J. Lewandowski, TMS Annual Meeting, San Diego, CA, March 1, 2017.

"New Insights into Environment Assisted Cracking of Pre-Exposed and Sensitized 5xxx Series Aluminum", T. Burnett, H. Holroyd, J.J. Lewandowski, and M. Seifi, Corrosion 2017, New Orleans, LA, March 27, 2017.

"Environmentally Enhanced Cracking in 5XXX Al-Mg Alloys", B. Palmer and J.J. Lewandowski, CWRU Research SHOWCASE, Cleveland, OH, April 21, 2017.

"Environmentally-Enhanced Cracking of 5XXX Al-Mg Alloys", B. Palmer and J.J. Lewandowski, MS&T 2017, Pittsburgh, PA, October 11, 2017.

2018
"Sensitization Effects on Environmentally-Assisted Cracking in 5XXX Al Alloys", J.J. Lewandowski, TMS Annual Mtg., Phoenix, AZ, March 12, 2018.

"Sensitization Effects on Tensile Behavior in 5XXX Series Aluminum Alloys", B. Palmer and J.J. Lewandowski, TMS Annual Mtg., Phoenix, AZ, March 15, 2018.

"Environmentally-Enhanced Cracking of 5XXX Al-Mg Alloys", B. Palmer and J.J. Lewandowski, CWRU Research SHOWCASE, Cleveland, OH, April 20, 2018.

**"Environmental Effects on Mechanical Reliability of Al-Mg 5XXX Alloys in Naval and Defense Applications" J.J. Lewandowski, Dept. Mechanical and Aerospace Engineering, SC3DP- Nanyang Technological University, Singapore, June 6, 2018.

"Extraction of EAC Crack Growth Rates and Stress Intensity Factors from Slow Strain Rate Test Data for 5XXX and 7XXX Series Aluminum Alloys", N.J.H. Holroyd, T. Burnett, B. Palmer, and J.J. Lewandowski, ECF Conference on Stress-Assisted Corrosion Damage, Hernstein, Austria, July 17, 2018.

Environmental Cracking in Al Ship Material", B. Palmer and J.J. Lewandowski, MS&T, Columbus, OH, October 15-18, 2018.

Papers published acknowledging N00014-15-1-2445

Seifi, S.M., Holroyd, N.J.H., and Lewandowski, J.J. (2016). "Deformation Rate and Sensitization Effects on Environmentally Assisted Cracking of Al-Mg Naval Alloys", Corrosion, 72(2), pp. 264-283.

Holroyd, NJ.H., Burnett, T.L., Seifi, M., and Lewandowski, J.J. (2017). "Improved Understanding of Environment-Induced Cracking (EIC) of Sensitized 5XXX Series Aluminum Alloys", Materials Science and Engineering A, 682, pp. 613-621.

Burnett, T.L., Holroyd, N.J.H., Lewandowski, J.J., Ogurreck, M., Rau, C., Kelly, R., Pickering, E.J., Daly, M., Sherry, A.H., Pawar, S., Slater, T.J.A., and Withers, P.J. (2017). "Degradation of Metallic Materials Studied by Correlative Tomography", in 38th Riso International Symposium on Materials Science – IOP Conf. Series: Materials Science and Engineering, 219, 021001.

Awards Received by PI and Students during 2015-2018 supported period:

PI Awards: John J Lewandowski
Nominee - John S. Diekhoff Award for Graduate Mentoring, CWRU (2017)
Los Alamos National Lab Institute for Materials Science Invited Seminar Speaker (2015)
Gordon Conference on Physical Metallurgy Speaker (2015)
Summer Visiting Professor-Singapore Center 3D Printing (SC3DP), Singapore (2015-present)

G Student Awards: Benjamin Palmer
- 2018 CWRU Research SHOWCASE Poster Award
- Honorable Mention – NSF Graduate Student Fellowship